Curvilinear Waveforms for Fluid Dispensing

J. E. Clark*

Zebra Technologies, Vernon Hills, IL, USA, jclark3@zebra.com
(*previously at PerkinElmer Life & Analytical Sciences, Downers Grove, IL, USA)

ABSTRACT

Piezoelectric micropipettes, a type of drop-on-demand ink jet microdispenser, are typically driven by repetitively pulsed waveforms to cause fluid ejection through a small orifice. To study the effect of drive waveform shape on drop ejection from these microdispensers, an arbitrary waveform generator was incorporated into a drop ejection visualization system. Among the drive waveforms investigated were several simple mathematical shapes, such as rectangular, trapezoidal, rectified and damped sine, and various waveform shapes defined by symmetric and asymmetric distribution functions, including Gaussian, Lorentzian, logistic, lognormal, Maxwell and Rayleigh distributions. Some of these waveforms are useful for extending the drop volume range over which satellite-free drop formation can be achieved.

Keywords: drop-on-demand, ink jet printing, fluid microdispenser, drop formation, drive waveform

1 INTRODUCTION

Piezoelectrically actuated micropipettes are used to generate microdrops of various fluids for a variety of non-contact microdispensing applications, such as miniaturized biological and chemical assays, security printing, micro-manufacturing of optic and electronic components, and precise application of special purpose liquids that have unique functional properties. Due to interactions between the electromechanical structure and material composition of the microdispenser, fluid cavity geometry and orifice shape parameters, physical and rheological properties of the fluid, applied pressure and drive waveform, various kinds of fluid ejection are possible, such as aerosol mists, sprays, drops or filaments. In typical microdispensing and ink jet printing applications, physical construction of the microdispenser is fixed, but fluid attributes can vary significantly according to the end users' application requirements. Thus, the drive waveform is a prime candidate for effecting and controlling stable fluid ejection modes [1].

2 DROP VISUALIZATION SYSTEM

Drop visualization systems are used to observe, record, and analyze microscopic images of drop ejection processes and subsequent flight trajectories from ink jet printheads and similar fluid microdispensing devices. Time-averaged and single event imaging systems for jet characterization and analysis are commercially available [2-4], and various specialized drop visualization and automated analysis systems have been developed for fluid jet research purposes [5-6].

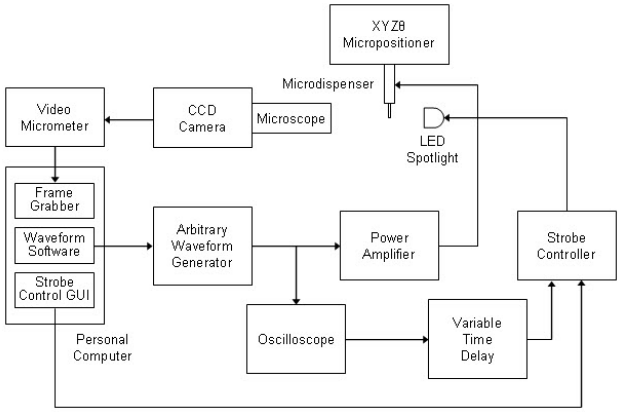

Figure 1: Drop visualization system block diagram.

The drop visualization system illustrated in Figure 1 was used to study the effect of various drive waveforms on jetting behavior of deionized water from piezoelectrically actuated micropipettes. The micropipette consists of a borosilicate glass capillary tube tapered at one end to form a nozzle as shown in Figure 2. A piezoelectric tube with radial polarization is coaxially bonded onto the glass capillary tube. This tubular assembly is housed within a protective sheath that provides both mechanical support and electrical isolation. The housing also contains electrical connections to a wideband power amplifier (Krohn-Hite 7600M) and arbitrary waveform generator (Pragmatic Instruments 2414B). When a positive voltage pulse is applied, the piezoelectric tube radially contracts in squeezer mode to cause drop ejection [7]. A pressure controller (not shown) maintains the microdispenser fluid supply constant at a low negative gauge pressure typically near -10 mbar.

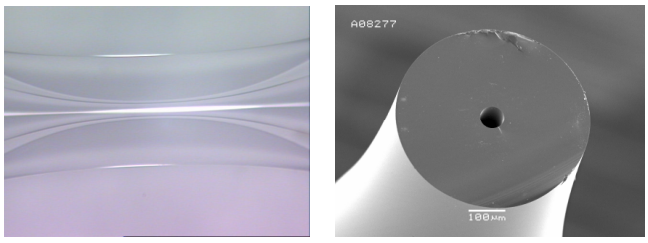

Figure 2: Tapered 70 µm nozzle before and after cleaving.

Curvilinear drive waveforms, as defined in sections 3.1 through 3.9, are created using Mathcad and uploaded from the PC to memory in the arbitrary waveform generator. To generate rectangular and trapezoidal waveforms, a precision pulse generator with adjustable rise and fall times was used instead of the arbitrary waveform generator.

Ejected drops are viewed with a high magnification microscope lens system (Navitar Zoom 6000) mounted onto a monochrome CCD camera. A 4-axis micropositioner enables precise location of the microdispenser and fluid jet within the field of view of the microscope and also permits spatial reference measurements used to calibrate the video micrometer. Still images and video clips are captured and saved with a PC-based frame grabber (Matrox Imaging).

Stroboscopic illumination for time-averaged imaging is provided by an LED spot light and strobe control system with PC-based graphical user interface (Advanced Illumination). Spatial position and temporal drop evolution are measured respectively with a video micrometer (Imagen XR-2000) and variable time delay, which is a built-in feature of the dual time base oscilloscope (Tektronix 2465B) used to monitor the drive waveform. The time delay signal also provides the input trigger signal for strobe synchronization.

3 CURVILINEAR WAVEFORMS

To generate curvilinear waveforms, a set of waveform points must be calculated on the personal computer, saved in a custom profile data file and uploaded to memory in the arbitrary waveform generator.

Curvilinear waveform points, which are defined in sections 3.1 through 3.9, use the following nomenclature:

$N + 1$	number of waveform elements
y_i	i^{th} data element for $i = 0, 1, 2, \ldots N$
A	amplitude (different for each waveform type)
n	integer number of half-periods
α	linear damping coefficient
β	linear damping constant
λ	exponential damping constant
μ	mean
σ	standard deviation
ω	full width at half amplitude
δ	shape factor
m	geometric mean
s	geometric standard deviation
κ	shape factor

Waveform names appearing in sections 3.1 through 3.9 are descriptive of their essential shapes and do not necessarily use the same normalization or have the identical functional form as their corresponding distribution functions in statistics and physics. Reverse waveforms, as defined in sections 3.7 through 3.9, are mirror images of their counterpart waveforms.

All waveforms are evaluated for the range, $i = 0, 1, 2, \ldots N$, except the lognormal waveforms in Eqs. (8) and (9), which span the range, $i = 1, 2, 3, \ldots N$. The number of waveform elements $N + 1$ is constrained by

$$N = t_d f_s \tag{1}$$

where t_d is the pulse duration and f_s is the sampling frequency of the arbitrary waveform generator.

3.1 Rectified Sine

$$y_i = A \sin\left(\frac{\pi}{N} i\right) \tag{2}$$

3.2 Linearly Damped Inverted Sine

$$y_i = A\left(\frac{\alpha}{N} i + \beta\right) \sin\left(\frac{n\pi}{N} i\right) \tag{3}$$

where $n \geq 3$ and $0 < \alpha \leq \beta$ and $\beta > 0$.

3.3 Exponentially Damped Inverted Sine

$$y_i = A \exp\left(-\frac{\lambda}{N} i\right) \sin\left(\frac{n\pi}{N} i\right) \tag{4}$$

where $n \geq 3$ and $\lambda > 0$.

3.4 Gaussian

$$y_i = A \exp\left[-\frac{(i-\mu)^2}{2\sigma^2}\right] \tag{5}$$

where $\mu = \frac{N}{2}$ and $\sigma \leq \frac{N}{7}$ are useful for waveforms of practical interest.

3.5 Lorentzian

$$y_i = \frac{A}{\left(\frac{i-\mu}{\frac{\omega}{2}}\right)^2 + 1} \tag{6}$$

NSTI-Nanotech 2009, www.nsti.org, ISBN 978-1-4398-1784-1 Vol. 3, 2009

where $\mu = \frac{N}{2}$ and $\omega \le \frac{N}{9}$ are useful for waveforms of practical interest.

3.6 Logistic

$$y_i = \frac{A \exp\left[-\left(\frac{i-\mu}{\delta}\right)\right]}{\left\{1+\exp\left[-\left(\frac{i-\mu}{\delta}\right)\right]\right\}^2} \qquad (7)$$

where $\mu = \frac{N}{2}$ and $\delta \approx \frac{N}{14}$ are useful for waveforms of practical interest.

3.7 Lognormal and Reverse Lognormal

$$y_i = \frac{A}{i^r}\exp\left[-\frac{(\ln i - \ln m)^2}{2(\ln s)^2}\right] \quad \text{and} \quad y_i = 0 \qquad (8)$$

$$y_{N-i} = \frac{A}{i^r}\exp\left[-\frac{(\ln i - \ln m)^2}{2(\ln s)^2}\right] \quad \text{and} \quad y_N = 0 \qquad (9)$$

where $r = 1$. Other values of $r \ge 0$ can be used to alter shape of the resulting waveform.

3.8 Maxwell and Reverse Maxwell

$$y_i = Ai^p \exp(-\kappa i^q) \qquad (10)$$

$$y_{N-i} = Ai^p \exp(-\kappa i^q) \qquad (11)$$

where $p = q = 2$ and $\kappa > 0$. Other values of $p > 0$ and $q > 0$ can be used to alter shape of the resulting waveform.

3.9 Rayleigh and Reverse Rayleigh

$$y_i = Ai^p \exp(-\kappa i^q) \qquad (12)$$

$$y_{N-i} = Ai^p \exp(-\kappa i^q) \qquad (13)$$

where $p = 1$, $q = 2$ and $\kappa > 0$. Other values of $p > 0$ and $q > 0$ can be used to alter shape of the resulting waveform.

4 ILLUSTRATIONS

The following drop ejection images represent some examples of the drop volume range that can be dispensed by the same microdispenser (70 μm nozzle diameter) when it is driven by several different drive waveforms.

All of the following figures depict satellite-free ejection of deionized water drops with drop speeds near 2 m/sec. Deionized water usually is a very difficult fluid to eject from drop-on-demand ink jet printheads owing to its high surface tension and low viscosity. This combination of physical properties favors jet evolution instabilities that can lead to excessive satellite drop formation with many fluid jetting devices. Viscosity and surface tension modifiers are commonly added to water based inks and functional fluids to improve their jetability. These images demonstrate that the drive waveform choice can also contribute to the prevention of undesirable satellite drop formation.

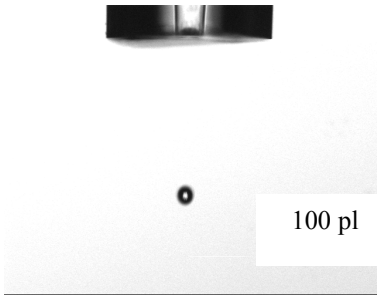

Figure 3: Exponentially damped inverted sine.

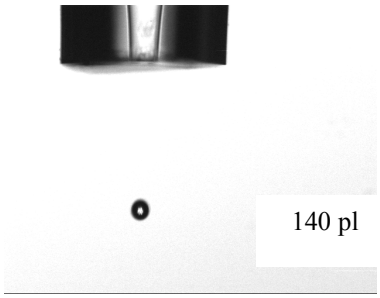

Figure 4: Lognormal.

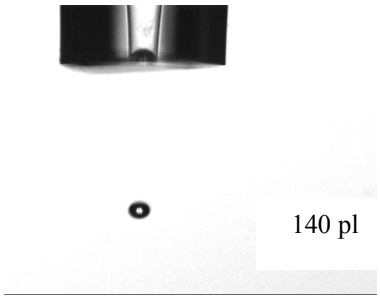

Figure 5: Reverse lognormal.

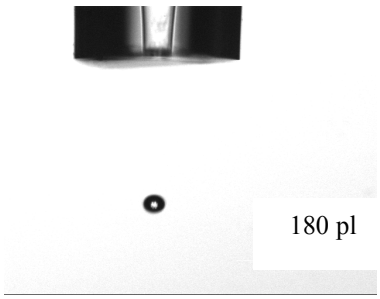

Figure 6: Rectified sine.

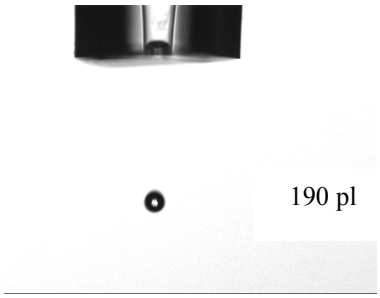

Figure 7: Gaussian.

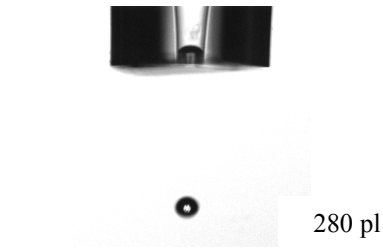

Figure 8: Reverse lognormal.

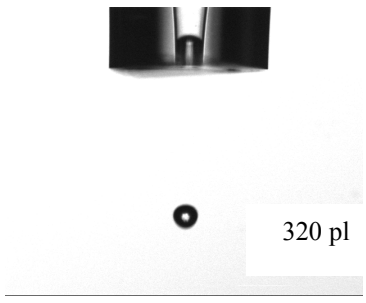

Figure 9: Rectangular.

In general, pulse amplitude and pulse duration for a specific drive waveform shape can be adjusted to provide satellite-free drop ejection over a bounded continuous range of drop volumes. For example, amplitude and duration of the reverse lognormal waveform defined in equation (9) were adjusted to provide satellite-free ejection of deionized water drops ranging in volume from 140 pl to 280 pl when ejected from the same piezoelectric micropipette at 2 m/sec. Drop ejection examples at the boundaries of the drop volume range for this drive waveform appear in Figures 5 and 8.

5 SUMMARY

Drop ejection characteristics of several drive waveform variants were studied, including rectangular, trapezoidal, damped and rectified sine, symmetric and asymmetric curvilinear shapes. Numerous regions of stable drop ejection were discovered by selecting the waveform type and then changing its shape in a controlled manner.

The drop volume range that can be achieved with the fluid, apparatus and drive waveform types described in this study is approximately 100 to 400 pl. Drop volumes are not necessarily continuously variable over this entire drop volume range and several different waveform types are needed to provide stable satellite-free drop ejection over sub-regions of this range.

This study suggests that a number of drive waveform types having adjustable waveform shape parameters could be implemented in a fluid dispensing controller to extend the drop volume range that can be dispensed with a given microdispenser in order to satisfy a potentially broader range of user applications.

6 ACKNOWLEDGEMENT

The author gratefully acknowledges PerkinElmer Life & Analytical Sciences for granting permission to present results of this drive waveform study. Related patent rights are assigned to PerkinElmer, Inc. [8].

REFERENCES

[1] E.R. Lee, "Microdrop Generation," CRC Press, 2002.
[2] www.imagexpert.com
[3] www.iticorp.com
[4] www.xennia.com
[5] A.U. Chen and O.A. Basaran, "A New Method for Significantly Reducing Drop Radius Without Reducing Nozzle Radius in Drop-On-Demand Production," Phys. Fl. 14(1), L1-L4, 2002.
[6] I.M. Hutchings, G.D. Martin, and S.D. Hoath, "High Speed Imaging and Analysis of Jet and Drop Formation," J. Imag. Sci. Tech. 51(5), 438-444, 2007.
[7] S.I. Zoltan, "Pulsed Droplet Ejecting System," U.S. Patent No. 3,857,049, 1974.
[8] J.E. Clark, "Method and Apparatus for Fluid Dispensing Using Curvilinear Drive Waveforms," U.S. Patent No. 7,357,471, 2008, and comparable international patents.